Shen *et al. Soft Sci* 2023;3:20
DOI: 10.20517/ss.2023.10

Soft Science

Research Article

Open Access

Check for updates

A lamellar-ordered poly[bi(3,4-ethylenedioxythiophene)-alt-thienyl] for efficient tuning of thermopower without degenerated conductivity

Lanlan Shen[1,3], Mengting Liu[2], Peipei Liu[1,2], Jingkun Xu[1,2,*], Na Li[2], Zhiliang Wan[2], Zhihong Chen[2], Congcong Liu[2,*], Weiqiang Zhou[2], Yuzhang Liang[3], Fengxing Jiang[2,*]

[1]Department of Physics, Jiangxi Science & Technology Normal University, Nanchang 330013, Jiangxi, China.
[2]Jiangxi Key Laboratory of Flexible Electronics, Jiangxi Science & Technology Normal University, Nanchang 330013, Jiangxi, China.
[3]College of Physis, Dalian University of Technology, Dalian 116024, Liaoning, China.

[*]**Correspondence to:** Profs. Fengxing Jiang, Jingkun Xu, Congcong Liu, Key Laboratory of Flexible Electronics, Jiangxi Science & Technology Normal University, 605 Fenglin Avenue, Economic and Technological Development Zone, Qingshanhu District, Nanchang 330013, Jiangxi, China. E-mail: f.x.jiang@live.cn; xujingkun@tsinghua.org.cn; lcc.0705@163.com

How to cite this article: Shen L, Liu M, Liu P, Xu J, Li N, Wan Z, Chen Z, Liu C, Zhou W, Liang Y, Jiang F. A lamellar-ordered poly[bi(3,4-ethylenedioxythiophene)-alt-thienyl] for efficient tuning of thermopower without degenerated conductivity. *Soft Sci* 2023;3:20. https://dx.doi.org/10.20517/ss.2023.10

Received: 27 Feb 2023 **First Decision:** 17 Mar 2023 **Revised:** 4 May 2023 **Accepted:** 18 May 2023 **Published:** 19 Jun 2023

Academic Editor: Zhi-Gang Chen **Copy Editor:** Lin He **Production Editor:** DongLi-Li

Abstract

Modulating the structural order of conjugated polymers has emerged as a significant approach to enhance the organic thermoelectric performance. Among these materials, poly(3,4-ethylenedioxythiophene) is considered a promising candidate due to its high conductivity. However, its low thermopower remains a major obstacle to further improve its performance as an organic thermoelectric material. To address this issue, a series of thiophene derivatives with high rigidity and containing dioxyethylene groups were synthesized, and polymer films were prepared through a simple and mild in-situ polymerization method. The polymer molecule containing a thiophene block, named poly[bi(3,4-ethylenedioxy)-alt-thienyl] , exhibits significant self-rigidification due to non-covalent interactions between oxygen and sulfur atoms, resulting in highly ordered assembly. By adding thiophene and thieno[3,2-b]thiophene structures to the intermediate precursor bi(3,4-ethylenedioxy), the 3,4-ethylenedioxy content in the polymer molecule is altered, leading to an almost four-fold increase in the thermopower of the thin film polymer and achieving a maximum thermopower of around 26 $\mu V \cdot K^{-1}$. Although poly[bi(3,4-ethylenedioxy)-alt-thienyl] shows a significant increase in thermopower compared to poly[bi(3,4-ethylenedioxy)], the thin film

conductivity exhibits a nearly imperceptible decreasing trend due to its highly ordered microstructure. This work highlights the potential to control the aggregation state of polymer molecules and achieve an approximate decoupling between the conductivity and thermopower of thermoelectric materials by rationally designing polymer molecules.

Keywords: Aggregation regulation, precursor structure modification, polythiophenyl derivatives, organic thermoelectric material

INTRODUCTION

Extensive efforts have been invested in comprehending the correlation between structure and performance, which has led to significant advancements in organic π-conjugated materials over the last two decades[1]. The design of molecular structure plays a crucial role in controlling the morphology and thermoelectric (TE) properties of materials, making π-conjugated polymers highly promising for use in TE generators[2]. Research has shown that the ordered structure of π-conjugated polymers, ranging from the molecular scale to the macroscale, significantly affects the properties of organic TE materials[3-7]. Within crystalline domains, the conjugation of molecular units leads to planar structures that orderly stack against each other (i.e., π stacking), resulting in close intermolecular contacts at the π-electronic levels, intermolecular electronic coupling, and effective charge transfer[7-12]. Reasonable structural design of precursor molecules, such as expanding the conjugated plane and introducing non-covalent interactions to promote self-rigidification of the conjugated backbone, can achieve control over the microscale ordered structure of polymer molecules to a certain extent. For instance, non-covalent interactions between atoms such as S, O, F and H can reduce the twisting angle between conjugated planes, promote ordered stacking of molecules, and optimize the spatial aggregation state of molecules[13-17]. Additionally, extending the conjugated backbone of the precursor is viewed as a convenient approach to narrow band gaps and regulate the electrical properties of organic conjugated materials[12,18-22].

At present, the substituents of thiophene (Th), thieno[3,2-b]thiophene (TT), and 3,4-ethylenedioxythiophene (EDOT) are commonly used as building blocks to extend the conjugation plane in organic electronic devices. TT, which is the simplest fused Th consisting of two annulated Th units, has more rigid and elongated π-conjugation structures than Th. This makes it a valuable tool for adjusting the band gap and enhancing intermolecular interactions in solid-state organic materials. Compared to Th, the presence of the dioxyethylene group in the EDOT structure can increase the charge density on the Th ring. This is beneficial for lowering the monomer oxidation potential and promoting effective doping of the polymer molecules. Imae *et al.* explored the effect of different proportions of EDOT units in polymer molecules on their electrochemical, optical, and electronic transport properties. They accomplished this by designing the structures of precursor molecules based on derivatives of polythiophene (PTh)[23,24]. Xue *et al.* designed and synthesized a series of binary or ternary precursors using components such as EDOT, Th, and TT. They studied the electrochemical and electrochromic properties of their monomers and polymers[23-27]. Poly(3,4-ethylenedioxythiophene) (PEDOT) is widely recognized as a leading organic TE material due to its environmental stability, broad conductivity (σ) range, and ability to be processed in solution[28]. However, the inadequate thermopower (S) of PEDOT has long impeded its widespread adoption as an organic TE material in the market[29-31]. In contrast, the Th and their derivatives generally have a higher S and a lower σ for PEDOT. It is important to note that the morphology and properties of the polymer film can vary significantly depending on the specific preparation techniques employed. Compared to the conventional chemical oxidation method, electrochemical polymerization produces PEDOT with a more uniform and continuous structure, resulting in an improvement of its σ by an order of magnitude[32-33]. Xiong *et al.* have demonstrated that well-ordered thin films of Poly(3,4-ethylenedioxythiophene):poly(styrenesulfonate)

(PEDOT:PSS) can be prepared using a commercially available material and a simple dilution filtration method[34]. Li *et al*. have successfully obtained PEDOT:PSS thin films with a power factor (*PF*) as high as 133 $\mu W \cdot m^{-1} \cdot K^{-2}$ using this method[35]. Since the discovery of classic conductive polymers, π-conjugated polymers have been a focus of attention in various organic electronic device fields due to their convenient structural modification and the close relationship between their structure and properties. However, modifying π-conjugated polymers often involves developing larger π-conjugated planar systems, which requires consideration of the poorer solution processability and film-forming performance caused by the introduction of large rigid structures. Hence, researchers must continue to explore a straightforward, dependable, and practical approach for producing polymer films from precursors with high rigidity structures. This requires continuous research and comprehension of the correlation between polymer molecular structure and performance, along with persistent exploration of advanced material preparation technology. As a result, the dimensionless figure of merit (ZT) value of organic TE materials has significantly expanded. However, earlier studies failed to consider the impact of microstructural aggregation state of polymer molecules on TE performance, leading to fragmented understanding of the relationship between polymer structure, properties, and microstructural aggregation state. Due to this lack of clarity, organic TE materials are currently unable to achieve large-scale commercial applications.

We have synthesized three monomers, according to the ^{1}H NMR spectra in Supplementary Figures 1-3, namely 2,2',3,3'-tetrahydro-5,5'-bithieno[3,4-b][1,4] dioxine (BED), 2,5-bis(2,3-dihydrothieno [3,4-b][1,4]dioxin-5-yl)thiophene (BED-T), and 2,5-bis(2,3-dihydrothieno[3,4-b][1,4]dioxin-5-yl) thieno[3,2-b] thiophene (BED-TT) by integrating the building units Th and TT into the EDOT block. The detailed synthesis procedures are presented in the Supplementary experimental section. We investigated the effects of changing the backbone conjugated structure of precursors on the preparation of polymer films, morphology, band gap, and TE performance. Our findings suggest that the introduction of Th units expands the conjugate plane of precursor molecules, which effectively promotes the ordered stacking of polymer molecules. This leads to decoupling between the σ and *S*, ultimately significantly improving the TE properties of the material.

RESULTS AND DISCUSSION

As our understanding of the relationship between structure and performance continues to advance, the synthesis of low-solubility, highly rigid polymers are becoming increasingly prevalent. However, this has presented a significant challenge in terms of film formation during polymer preparation, and conventional methods may not be sufficient to achieve high-quality polymer films. The rigidity of BEDs molecules [Supplementary Scheme 1] further complicates this task, making it even more difficult to obtain high-quality polymer films[36,37] .To overcome the film quality problem for conjugated polymers, we propose a novel method for preparing high-quality films using the spray-spin coating method for polymerization[38], as illustrated in Figure 1. In this method, the monomer solution is atomized by an extremely fine atomizer and uniformly deposited on a substrate coated with a thin film of oxidizing agent. The monomer solution immediately reacts with the oxidizing agent, and high-quality polymer films are obtained after ethanol rinsing. Detailed film preparation steps are presented in the polymerization of BEDs monomers and polymer films preparation section of the Supplementary Material. By using a precursor with a large π-conjugate structure, we are able to achieve high-quality polymer preparation through a simple and low-cost solution treatment method. This opens potential applications in the field of photoelectricity.

To determine the coupling mode during precursor polymerization, we conducted Fourier transform infrared (FTIR) spectroscopy on the PBEDs films [Here, we define PBEDs as a group of polymer PBED, P(BED-T) and P(BED-TT)]. Supplementary Figure 4 shows that there are hardly any absorption peaks near 3,000-3,100 cm^{-1} (which were not depicted in the graph), corresponding to the C-H bond vibration at the 2

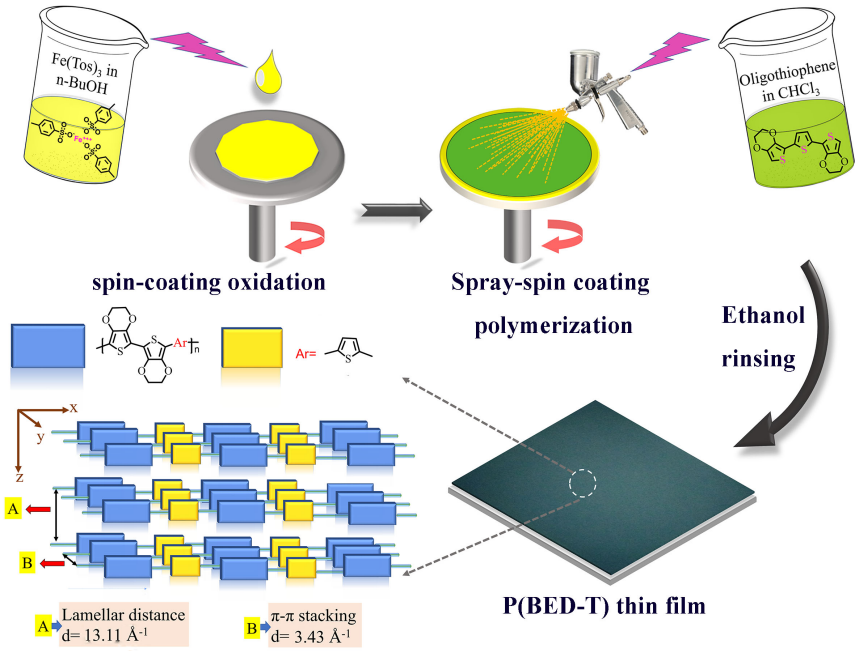

Figure 1. The schematic of the preparation of PBED, P(BED-T), and P(BED-TT) films. BED-T: 2,5-bis(2,3-dihydrothieno[3,4-b][1,4]dioxin-5-yl)thiophene; BED-TT: 2,5-bis(2,3-dihydrothieno[3,4-b][1,4]dioxin-5-yl)thieno[3,2-b]thiophene.

and 5 position on the Th ring[39]. This indicates that the polymerization reaction mainly occurred at the α position of the conjugated Th. Additionally, we observed absorption bands for the stretching vibration of the C=C bond in the Th ring at 1,513 cm^{-1}[40]. This suggests that the polymerization process did not involve any ring-opening reactions. In summary, our results demonstrate that we have successfully produced reliable PBEDs films.

The impact of introducing thienyl on the quality of PBEDs were evaluated by comparing their macroscopic uniformity and micro-roughness. Figure 2A-C indicates that PBEDs exhibit excellent uniform continuity, indicating that the addition of thienyl groups to the precursor does not affect the homogeneous continuity of the polymer film. This finding suggests that the spray-spin coating polymerization technique is a highly effective strategy for preparing high-quality films of precursor molecules with large conjugated rigid structures. Furthermore, we used atomic force microscopy (AFM) to analyze the morphology of PBEDs films and quantify the change in surface flatness caused by the introduction of thienyl groups. Figure 2D-F depict the topography of PBED, P(BED-T), and P(BED-TT) films, respectively. No differences in their aggregation at the topographic level were observed. Interestingly, the root-mean-square roughness (R_{ms}) of PBED, P(BED-T), and P(BED-TT) films were measured to be 49.4 nm, 26.9 nm, and 16.8 nm, respectively. This indicates a decrease in the R_{ms} of PBEDs film with the introduction of a larger conjugated structure of thienyl. The observed result is attributed to the introduction of larger conjugated structures, which increase the effective conjugated length of polymer molecules and promote their planar packing. Additionally, the non-covalent intermolecular and intramolecular interactions of O and S atoms of EDOT and Th or TT tend to give the polymer molecules a one-dimensional planar structure. The line profile graphs and large scanning areas of 80 μm × 80 μm, as shown in Figure 2G-I and Supplementary Figure 5, respectively, support the results of the above analysis.

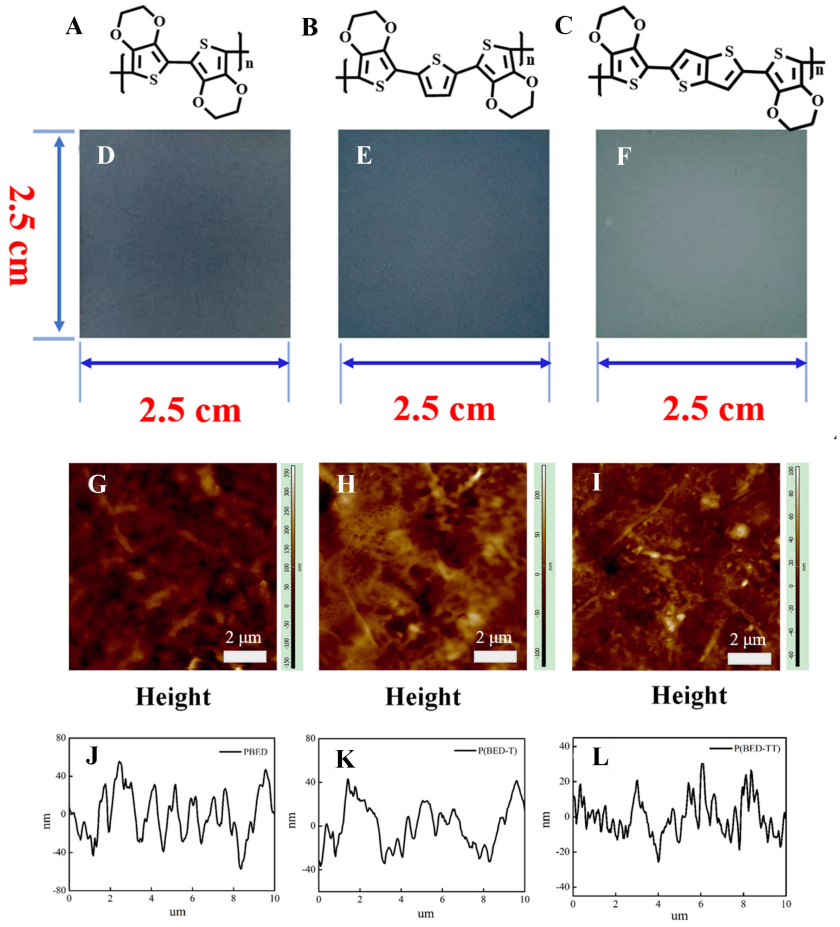

Figure 2. Figure 2A-C, D-F and G-I are digital photos, AFM morphology images and line profile graphs of AFM morphology of PBED, P(BED-T), P(BED-TT) films prepared by spray-spin coating polymerization method, respectively. Notes: the insets in Figure 2A-C shows the chemical structure corresponding to the PBEDs film and AFM morphology image of films scan area is 10 μm × 10 μm. AFM: atomic force microscopy; BED-T: 2,5-bis(2,3-dihydrothieno[3,4-b][1,4]dioxin-5-yl)thiophene; BED-TT: 2,5-bis(2,3-dihydrothieno[3,4-b][1,4]dioxin-5-yl)thieno[3,2-b]thiophene.

It is widely acknowledged that the electronic transport performance in classic semicrystalline polymers, such as PEDOT, poly(3-hexylthiophene-2,5-diyl) (P3HT), and poly(2,5-bis(3-alkylthiophene-2-yl) thieno[3,2-b] thiophenes) (PBTTT), is primarily determined by the long-range order[41-44]. To gain a better understanding of this phenomenon, the molecular stacking of PBEDs films was analyzed using grazing-incidence wide-angle X-ray scattering (GIWAXS), as depicted in Figure 3. The results reveal that both PBED and P(BED-T) molecules exhibit a combination of face-on (π-π stacking) and edge-on (lamellar stacking) mixed stacking modes, with an edge-on orientation. Notably, the P(BED-T) film demonstrates stronger crystallinity compared to PBED, indicating that the self-assembly behavior of the polymer molecules can be improved by introducing Th to increase the effective conjugation length of the monomer. Additionally, the (010) peaks of PBED and P(BED-T) are observed at Q_z = 1.78 Å^{-1} and 1.83 Å^{-1}, respectively, corresponding to *d*-spacing of 3.52 Å and 3.43 Å, as shown in Figure 3D. These results demonstrate that the polymer with Th exhibits a smaller π-π stacking distance and stronger backbone coupling compared to PBED. This can be attributed to the introduction of Th, which has a conjugated planar structure that enhances the conjugate plane of the entire polymer molecule. Figure 3E shows a third peak at around 1.25 Å^{-1}, which can be assigned to the (300) diffraction. However, the low intensity of this peak indicates that

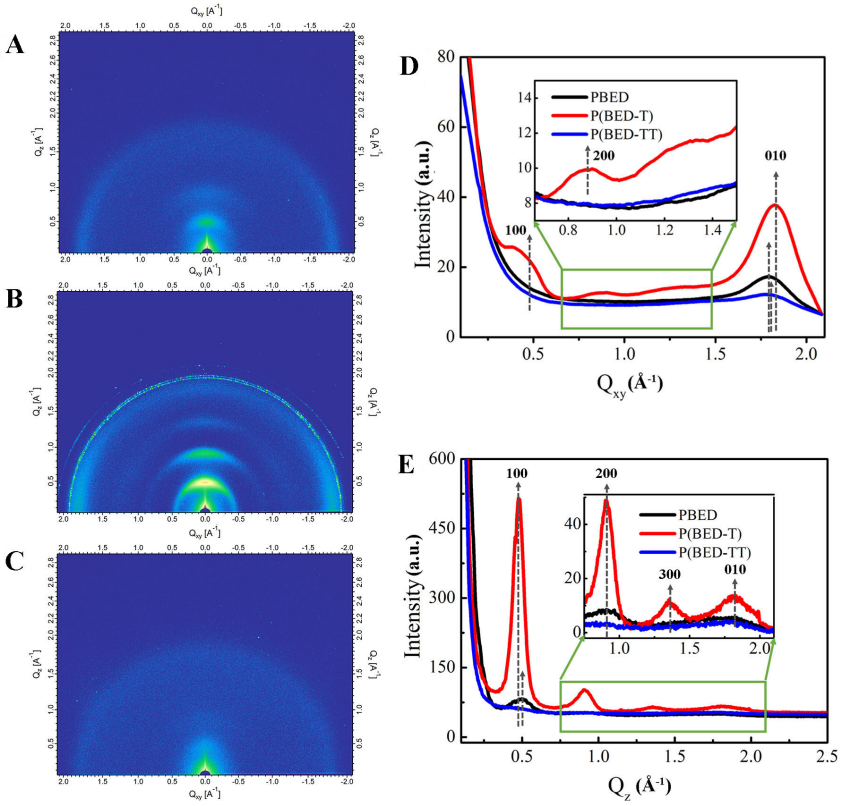

Figure 3. GIWAXS pattern of (A) PBED, (B) P(BED-T), and (C) P(PBED-TT) films; (D) in plane and (E) out-of-plane line-cuts in GIWAXS pattern of PBEDs films.

there is only a finite long-range order along the *z*-axis. This is due to the weak non-covalent bond between the O-S atoms of the EDOT and Th block, which reduces the effect of steric hindrance caused by the introduction of Th, increases the coplanarity of the polymer molecules and promotes the orderly stacking of polymer molecules. However, the introduction of the TT structure clearly alters the polymer molecules from their original ordered layered structure to a completely disordered amorphous structure in the 2D GIWAXS pattern and scattering intensity. This may be due to the increased rigidity of the monomer resulting from the introduction of the TT rigid structure, which limits the weight growth of the polymer molecules and reduces their effective conjugation length, making it unfavorable for the crystallization of the polymer molecules[31,45,46].

Furthermore, the PBEDs film exhibited ordered regions, and the incorporation of the Th structure enhanced the long-range ordered packing of polymer molecules, as confirmed by high resolution transmission electron microscopy (HRTEM) [Figure 4]. Interestingly, the P(BED-TT) film also displayed some ordered stacking regions and electron scattering signals, as shown in Figure 4C and F. However, unlike the long-range ordered stacking of P(BED-T) [Figure 4B and E], the ordered region of P(BED-TT) had a smaller network structure. This finding contradicts the results of GIWAXS characterization, which may be due to the unique short-range ordered network structure of P(BED-TT) that is not sufficient to yield prominent signal peaks in GIWAXS characterization. Therefore, these results suggest that the introduction of a Th block can promote the long-range ordered stacking of polymer molecules, while the incorporation

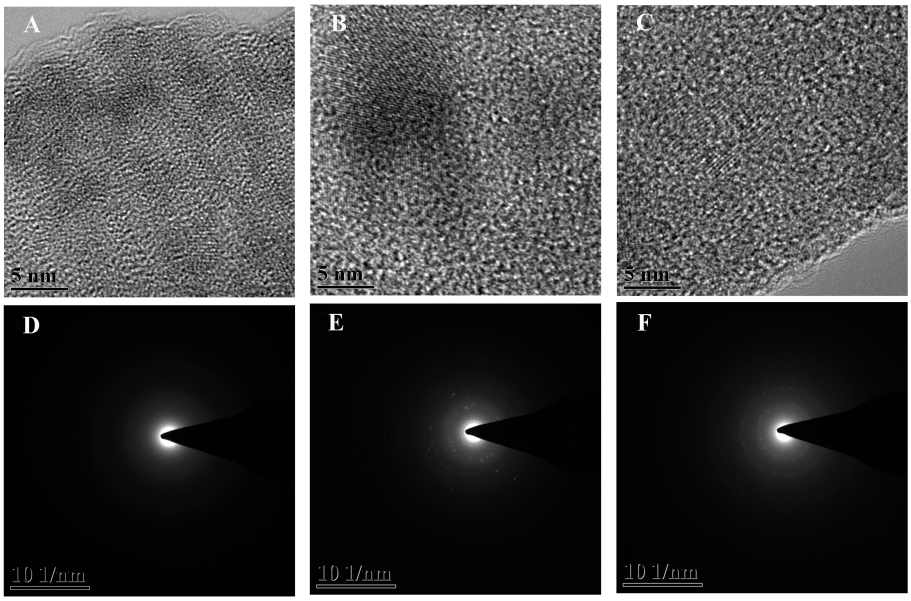

Figure 4. HRTEM images of (A), (D) PBED, (B), (E) P(BED-T) and (C), (F) P(BED-TT) films.BED-T: 2,5-bis(2,3-dihydrothieno[3,4-b][1,4]dioxin-5-yl)thiophene; BED-TT: 2,5-bis(2,3-dihydrothieno[3,4-b][1,4]dioxin-5-yl)thieno[3,2-b]thiophene; HRTEM:confirmed by high resolution transmission electron microscopy.

of an excessively rigid structure such as TT can lead to the realization of a short-range ordered network structure. It is well established that the long-range ordering of the majority of polymer molecules can significantly enhance carrier transport compared to the short-range ordered packing structure. Increasing carrier mobility is a crucial strategy for improving the σ of TE materials.

In addition, doping serves as a crucial method for regulating the properties of TE materials. By adjusting the degree of doping, the carrier concentration of the material can be effectively regulated, ultimately leading to the optimal value of σ and S[29]. To assess the doping level of semiconducting materials, ultraviolet-visible (UV-vis) absorption spectra are commonly used. In this study, we analyzed the UV-vis spectra of PBEDs films [Figure 5] and observed a significant absorption peak after approximately 600 nm, which is associated with the polaron and/or dipolaron subgap transition in the polymers[47,48]. This finding suggests that the BEDs monomers were effectively doped with the counter anions in the oxidant during the polymerization process. Notably, the incorporation of Th and TT altered the EDOT content of the polymer molecule, resulting in significant differences in the doped polymer molecules. Specifically, both P(BED-T) and P(BED-TT) exhibited pronounced absorption peaks at around 800 nm, whereas PBED displayed a broad and large absorption peak after 600 nm. Moreover, compared to PBED and P(BED-T), the neutral-state absorption peak of the π-π* transition nearly disappeared after doping in P(BED-TT), which still exhibited a neutral-state absorption peak at around 500 nm[49]. This observation may be attributed to the introduction of the TT unit, which significantly reduced the electron cloud density within the polymer molecule[23,24], thereby decreasing the degree of doping in the polymer molecule.

To further investigate the effect of extending the conjugate plane by introducing thienyl groups on the electrical properties of monomers and polymers, the correlation between molecular structure and electrical properties was considered. The anodic polarization curve of Figure 6A inset reveals that the initial oxidation potential (E_{ox}) of BED is significantly lower than that of EDOT (E_{ox} = 1.2 V, as shown in Supplementary Figure 6), reaching 0.57 V. This is mainly attributed to the increased effective conjugated chain length of the

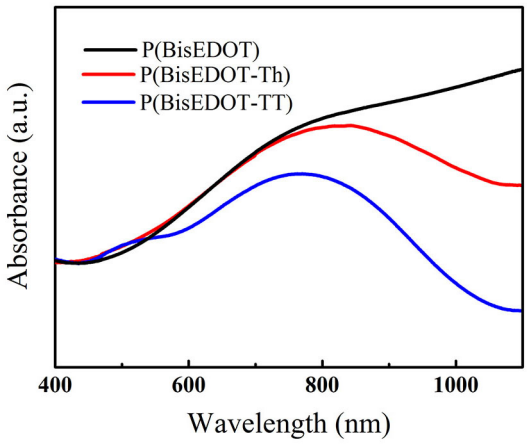

Figure 5. UV-vis absorption spectra of PBED, P(BED-T), P(BED-TT) films by spray-spin coating polymerization method. P(BED-TT) films. BED-T: 2,5-bis(2,3-dihydrothieno[3,4-b][1,4]dioxin-5-yl)thiophene; BED-TT: 2,5-bis(2,3-dihydrothieno[3,4-b][1,4]dioxin-5-yl)thieno[3,2-b]thiophene.

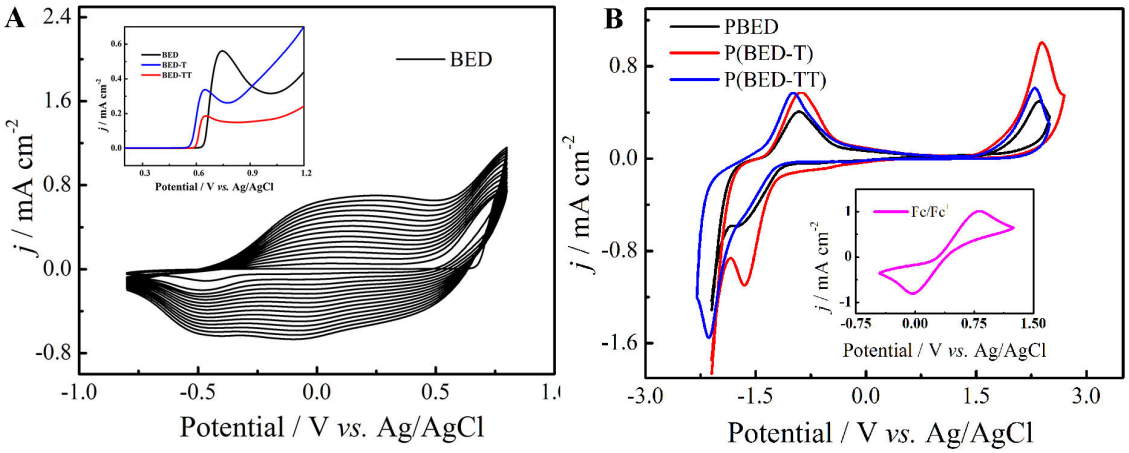

Figure 6. (A) Cyclic voltammetry curve of 0.01M BED in PC/$LiClO_4$. Potential scan rate: 50 $mV \cdot s^{-1}$. Inset: Anodic oxidation curves of 0.01 M BED (black), BED-T (blue) and BED-TT (red) in PC/$LiClO_4$. Potential scan rate: 10 $mV \cdot s^{-1}$; (B) Cyclic voltammetry curve of PBED, P(BED-T), and P(BED-TT); the inset shows the cyclic voltammogram of ferrocene/ferrocenium (Fc/Fc^+) couple used as an internal reference, and its E_{ox} is 0.27 V in our measure system.BED-T: 2,5-bis(2,3-dihydrothieno[3,4-b][1,4]dioxin-5-yl)thiophene; BED-TT: 2,5-bis(2,3-dihydrothieno[3,4-b][1,4]dioxin-5-yl)thieno[3,2-b]thiophene.

BED monomer. Moreover, the effective conjugation length of the monomers increases further with the introduction of Th and TT, resulting in lower E_{ox} values for BED-T and BED-TT. It is worth noting that the E_{ox} value of BED-TT is slightly higher than that of BED-T. This suggests that BED-TT has a smaller effective conjugate length compared to BED-T, due to the existence of a larger twist angle between the TT and EDOT conjugate structure compared to BED-T. Additionally, the cyclic voltammetry curve studies [Figure 6A and Supplementary Figure 7] demonstrate that BEDs exhibit good redox activities, and the redox reversibility is not significantly affected by the introduction of thienyl groups.

In addition, it should be noted that the energy levels of polymers can have a significant impact on their photoelectric properties, and the size of the band gap is closely related to their chemical structure. Therefore, we conducted an analysis of the electrochemical energy bands and optical bands of PBEDs

[Figure 6B and Table 1]. The PBEDs films exhibited deep highest occupied molecular orbital (HOMO) levels, with onset oxidation and reduction potentials estimated to be less than -6 eV, which is significantly deeper than PEDOT's -5.1 eV[3]. This difference could be attributed to the more rigid structure of PBED precursors, resulting in fewer repeating units compared to PEDOT[50-53]. Furthermore, the UV-vis absorption spectra of PBEDs films after de-doping with hydrazine hydrated ethanol solution were analyzed and presented in Supplementary Figure 8. The absorption spectra of PBEDs showed strong absorption in the 400-700 nm region. Notably, the absorption spectrum of P(BED-T) exhibited a blue shift phenomenon, while P(BED-TT)'s had a slight red shift. The difference in the maximum absorption peak position of the PBEDs film may be due to the variation in intermolecular π-π stacking interaction between these polymers[54]. Additionally, the optical bandgap of PBEDs was estimated by absorption edge and presented in Table 1. The results showed that the optical band gap of the PBEDs film was very small, ranging between 1.73-1.78 eV, demonstrating that the incorporation of thienyl groups minimally affected the energy band of PBEDs.

Figure 7 illustrates the density functional theory (DFT) calculation of the BEDs trimer, revealing that the lowest occupied molecular orbital (LUMO) level of the polymer experiences a significant impact upon the incorporation of thienyl groups, leading to an increase in its electronic affinity. The results indicate that the introduction of thienyl groups can reduce the intramolecular charge density, resulting in a decrease in the effective doping degree with dopant molecules. In Figure 8, the incorporation of Th results in a reduction of the distortion angle between conjugate planes from 1.25° to 0.62° and 0.57° by utilizing non-covalent forces between O and S atoms. Furthermore, a distinct twist angle of the conjugated plane is observed, with the embedded TT structure resulting in a larger change in the twist angle compared to the introduction of the Th structure. This could be due to the rigid structure and steric hindrance of the TT structure, which affects the overall conformation of the molecule. This phenomenon is consistent with the precursor E_{ox} electrochemical characterization and validates the results of GIWAXS characterization. Notably, the electron cloud of the polymer is mainly distributed on the conjugated ring. However, upon introducing thienyl groups, the distribution of electron clouds on the conjugated main chain of the molecule becomes relatively uneven and aggregates towards the center when compared to PBED. This effect is more pronounced in P(BED-TT).

The TE properties of PBEDs films were measured using a standard four-point probe technique. As shown in Figure 9A, the embedding of the Th structure had a relatively small impact on the σ of the polymer film compared to the PBED film. The GIWAXS and HRTEM characterization of the films suggest that the slight decrease in film σ may be attributed to the ordered stacking of P(BED-T) molecules, which promotes carrier mobility. On the other hand, the embedding of the TT structure in the P(BED-TT) film resulted in a significant decrease in its σ due to the absence of apparent long-range ordered stacking of molecules. The embedding of the Th and TT structures resulted in a decrease in the proportion of EDOT units in the polymer molecules, which reduced the charge density on the polymer molecules, leading to a lower HOMO energy level and unfavorable effective doping. Consequently, the *S* of P(BED-T) and P(BED-TT) showed a significant increase, approximately four times that of the *S* of the PBED film.

To further optimize the TE performance of P(BED-T) films, we annealed the polymer films to release intermolecular stress and promote the free stretching of polymer and dopant molecules, thereby further optimizing the ordered stacking of polymer molecules. Figure 9B illustrates the impact of different annealing durations on the TE performance of the films. The TE performance of the films was optimized after annealing for 10 minutes at 120 °C in air, reaching 14.9 $\mu W \cdot m^{-1} \cdot K^{-2}$. This represents a nearly 50% increase in the *PF* compared to before annealing. Surprisingly, high temperature annealing in air led to a

Table 1. Optical and electrochemical data of PBED, P(BED-T), P(BED-TT)

Molecules	E_{red} (V)[a]	E_{ox} (V)[b]	[c]H^{ELE}/[d]H^{DFT} [eV]	[c]L^{ELE}/[d]L^{DFT} [eV]	$\lambda_{edge}^{fil.}$ [nm]e	$E_g^{opt.}$ [eV]f
PBED	-1.18	1.60	-6.10/-4.18	-3.35/-1.72	717	1.73
P(BED-T)	-1.23	1.58	-6.08/-4.18	-3.30/-2.06	698	1.77
P(BED-TT)	-1.12	1.85	-6.30/-4.35	-3.41/-2.18	685	1.78

[a]the E_{red} and [b]E_{ox} were observed by the cyclic voltammograms of PBEDs. [c]the H^{ELE} and L^{ELE} represent HOMO and LUMO energy levels measured by electrochemical methods, respectively, and energy level were carried out by the equation $E_{HOMO/LUMO}$ = - [E_{ox} - $E_{1/2}$(ferrocene) + 4.8], where *E*ox is the onset oxidation potential of the polymer, and $E_{1/2}$(ferrocene) is the half peak potential of ferrocene vs Ag/Ag^+. [d]the H^{DFT} and L^{DFT} represent HOMO and LUMO energy level measured by DFT calculation. [e]absorption edge $\lambda_{edge}^{fil.}$ of the conducting polymer films in the UV-Vis absorption spectra. [f]the values of $E_g^{opt.}$ were calculated based on the formula of $E_g^{opt.}$ = 1240 / $\lambda_{edge}^{fil.}$.

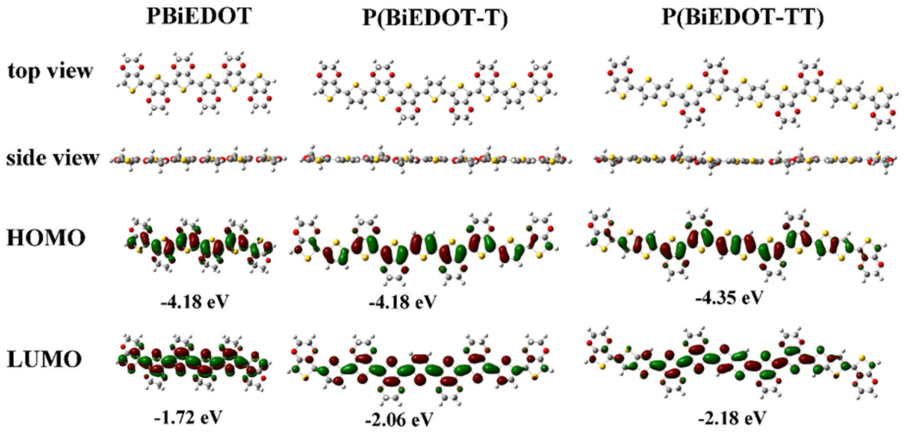

Figure 7. Chain conformations of designed PBEDs were expected from their trimer's conformation calculation under minimized energy state, and their dimer's electron distributions both in HOMO/LUMO state are illustrated. HOMO: Highest occupied molecular orbital; LUMO: lowest occupied molecular orbital.

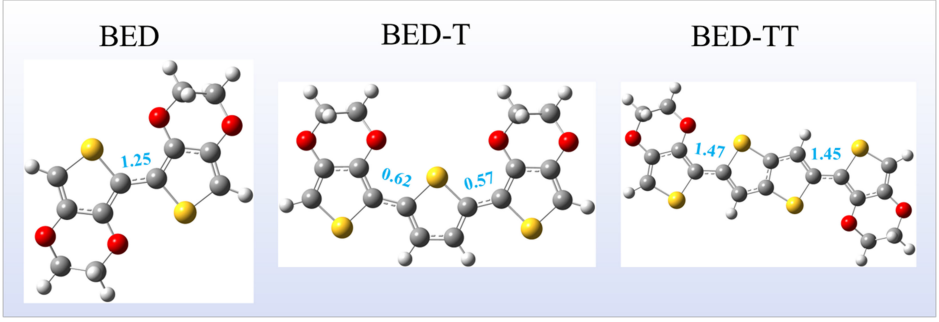

Figure 8. Molecular models of BED, BED-T and BED-TT fragments (calculated with DFT/B3LYP/6-31G method). BED-T showed more planar backbone than BED and BED-TT due to the nonbonding. BED: interactions.2,2',3,3'-tetrahydro-5,5'-bithieno[3,4-b][1,4]dioxine; BED-T: 2,5-bis(2,3-dihydrothieno[3,4-b][1,4]dioxin-5-yl)thiophene; BED-TT: 2,5-bis(2,3-dihydrothieno[3,4-b][1,4]dioxin-5-yl)thieno[3,2-b]thiophene.

significant decrease in the σ of the polymer film, while the *S* value increased significantly. There are two possible reasons for this phenomenon. Firstly, the high temperature annealing of the PBEDs film in air may cause oxygen in the air to react with the Th derivative chain, partially converting the double (π) bonds to single bonds[55]. This reaction increases the electron affinity of the polymer molecules and reduces the doping efficiency between the polymer molecules and the dopant. Additionally, since p-toluene sulfonic

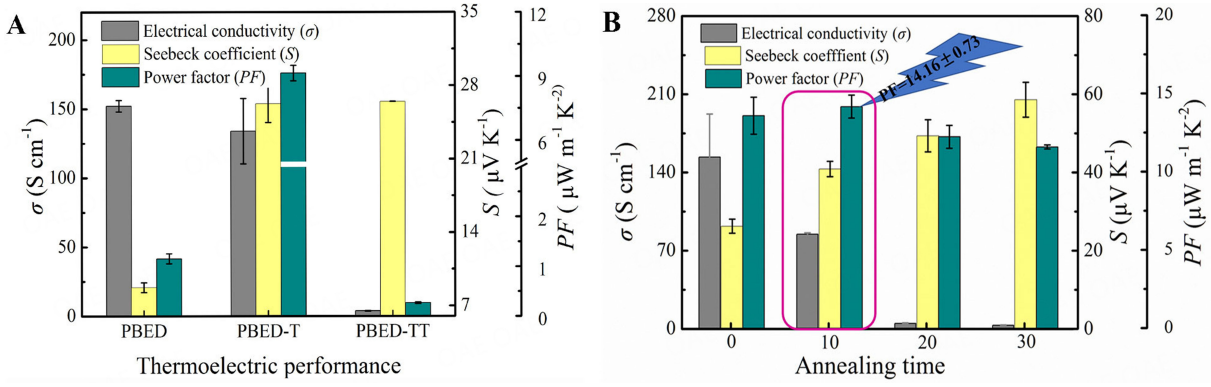

Figure 9. (A) TE parameters of PBEDs films that as-prepared directly by spray-spin coating polymerization method; (B) annealing time dependence of σ,*S* and *PF* of the P(BED-T) film at 120 ºC.TE:thermoelectric; BED-T: 2,5-bis(2,3-dihydrothieno[3,4-b][1,4]dioxin-5-yl)thiophene.

acid ions were used as dopants, and the boiling point of *p*-toluene sulfonic acid is around 116 ºC, a small amount of dopant may evaporate from the film during annealing at 120 ºC. This leads to the phenomenon of de-doping the polymer, resulting in a decrease in σ and an increase in the *S* value.

CONCLUSIONS

In conclusion, modifying the conjugated structure of BED led to the synthesis of three types of p-type polymers, whose microscopic aggregation and TE properties were studied. The embedding of Th and TT structures did not affect the homogeneous continuity of polymer films. However, it did reduce the content of EDOT within the polymer molecules, leading to a lower HOMO energy level and reduced doping efficiency of the dopant. As a result, both P(BED-T) and P(BED-TT) exhibited nearly fourfold increase in *S* values compared to PBED. The non-covalent interactions between S and O flattened the polymer molecule, promoted ordered assembly of polymer molecules, and enhanced the migration efficiency of charge carriers. After embedding the Th structure, the σ was not significantly reduced, achieving the decoupling of σ and *S*. These findings highlight the importance of understanding the relationship between polymer molecular structure, microstructure, aggregation structure, and properties for the preparation of high-performance TE materials.

DECLARATIONS

Authors' contributions

Made substantial contributions to conception and design of the study and performed data analysis and interpretation: Shen L, Jiang F, Xu J, Liu C, Liu M

Performed data acquisition, as well as provided administrative, technical, and material support: Shen L, Liu M, Liu P, Li N, Wan Z, Chen Z, Zhou W, Liang Y

Availability of data and materials

Not applicable.

Financial support and sponsorship

This work supported by the National Natural Science Foundation of China (No. 52073128, No. 52272214, and No. 22065013), the National Key Research and Development Program of China (No. 2022YFB3803900), the Natural Science Foundation of Jiangxi Province (No. 20203AEI003 and No. 20204BCJL22040), and Jiangxi Provincial Department of Education (No. GJJ2201334).

Conflicts of interest

All authors declared that there are no conflicts of interest.

Ethical approval and consent to participate

Not applicable.

Consent for publication

Not applicable.

REFERENCES

1. Wang S, Zuo G, Kim J, Sirringhaus H. Progress of conjugated polymers as emerging thermoelectric materials. *Prog Polym Sci* 2022;129:101548. DOI
2. Kaloni TP, Giesbrecht PK, Schreckenbach G, Freund MS. Polythiophene: from fundamental perspectives to applications. *Chem Mater* 2017;29:10248-83. DOI
3. Russ B, Glaudell A, Urban JJ, Chabinyc ML, Segalman RA. Organic thermoelectric materials for energy harvesting and temperature control. *Nat Rev Mater* 2016;1:16050. DOI
4. Zhou X, Pan C, Gao C, et al. Thermoelectrics of two-dimensional conjugated benzodithiophene-based polymers: density-of-states enhancement and semi-metallic behavior. *J Mater Chem A* 2019;7:10422-30. DOI
5. Lee M, Jeon H, Jang M, Yang H. A physicochemical approach toward extending conjugation and the ordering of solution-processable semiconducting polymers. *ACS Appl Mater Interfaces* 2016;8:4819-27. DOI
6. See KC, Feser JP, Chen CE, Majumdar A, Urban JJ, Segalman RA. Water-processable polymer-nanocrystal hybrids for thermoelectrics. *Nano Lett* 2010;10:4664-7. DOI PubMed
7. Chabinyc M. Thermoelectric polymers: behind organics' thermopower. *Nat Mater* 2014;13:119-21. DOI PubMed
8. Kang S, Jeffrey Snyder G. Charge-transport model for conducting polymers. *Nat Mater* 2017;16:252-7. DOI PubMed
9. Noriega R, Rivnay J, Vandewal K, et al. A general relationship between disorder, aggregation and charge transport in conjugated polymers. *Nat Mater* 2013;12:1038-44. DOI
10. Kawabata K, Osaka I, Nakano M, Takemura N, Koganezawa T, Takimiya K. Thienothiophene-2,5-Dione-based donor-acceptor polymers: improved synthesis and influence of the donor units on ambipolar charge transport properties. *Adv Electron Mater* 2015;1:1500039. DOI
11. Wang X, Sun Y, Chen S, et al. Effects of π-conjugated bridges on photovoltaic properties of donor-π-acceptor conjugated copolymers. *Macromolecules* 2012;45:1208-16. DOI
12. Cinar ME, Ozturk T. Thienothiophenes, dithienothiophenes, and thienoacenes: syntheses, oligomers, polymers, and properties. *Chem Rev* 2015;115:3036-140. DOI PubMed
13. Zheng YQ, Lei T, Dou JH, et al. Strong electron-deficient polymers lead to high electron mobility in air and their morphology-dependent transport behaviors. *Adv Mater* 2016;28:7213-9. DOI
14. Bardagot O, Kubik P, Marszalek T, et al. Impact of morphology on charge carrier transport and thermoelectric properties of N-type fbdopv-based polymers. *Adv Funct Mater* 2020;30:2000449. DOI
15. Mcentee GJ, Skabara PJ, Vilela F, et al. Synthesis and electropolymerization of hexadecyl functionalized bithiophene and thieno[3,2- *b*]thiophene end-capped with EDOT and EDTT units. *Chem Mater* 2010;22:3000-8. DOI
16. Son SY, Lee GY, Kim S, et al. Control of crystallite orientation in diketopyrrolopyrrole-based semiconducting polymers via tuning of intermolecular interactions. *ACS Appl Mater Interfaces* 2019;11:10751-7. DOI
17. Babudri F, Farinola GM, Naso F, Ragni R. Fluorinated organic materials for electronic and optoelectronic applications: the role of the fluorine atom. *Chem Commun* 2007:1003-22. DOI PubMed
18. de Silva KMN, Hwang E, Serem WK, Fronczek FR, Garno JC, Nesterov EE. Long-chain 3,4-ethylenedioxythiophene/thiophene oligomers and semiconducting thin films prepared by their electropolymerization. *ACS Appl Mater Interfaces* 2012;4:5430-41. DOI PubMed
19. Dou L, Liu Y, Hong Z, Li G, Yang Y. Low-Bandgap near-ir conjugated polymers/molecules for organic electronics. *Chem Rev* 2015;115:12633-65. DOI
20. Kim J, Park JB, Jung IH, et al. Well-controlled thieno[3,4-c]pyrrole-4,6-(5H)-dione based conjugated polymers for high performance organic photovoltaic cells with the power conversion efficiency exceeding 9%. *Energy Environ Sci* 2015;8:2352-6. DOI
21. Hwang H, Sin DH, Kulshreshtha C, et al. Synergistic effects of an alkylthieno[3,2-b]thiophene π-bridging backbone extension on the photovoltaic performances of donor-acceptor copolymers. *J Mater Chem A* 2017;5:10269-79. DOI
22. Cai P, Chen Z, Zhang L, Chen J, Cao Y. An extended π-conjugated area of electron-donating units in D-A structured polymers towards high-mobility field-effect transistors and highly efficient polymer solar cells. *J Mater Chem C* 2017;5:2786-93. DOI

23. Imae I, Ogino R, Tsuboi Y, Goto T, Komaguchi K, Harima Y. Synthesis of EDOT-containing polythiophenes and their properties in relation to the composition ratio of EDOT. *RSC Adv* 2015;5:84694-702. DOI
24. Imae I, Koumoto T, Harima Y. Thermoelectric properties of polythiophenes partially substituted by ethylenedioxy groups. *Polymer* 2018;144:43-50. DOI
25. Xue Y, Xue Z, Zhang W, et al. Enhanced electrochromic performances of Polythieno[3,2-b]thiophene with multicolor conversion via embedding EDOT segment. *Polymer* 2018;159:150-6. DOI
26. Xue Y, Xue Z, Zhang W, et al. Thieno[3,2- *b*]Thiophene end-capped all-sulfur analog of 3,4-ethylenedioxythiophene and its eletrosynthesized polymer: is distorted conformation not suitable for electrochromism? *J Polym Sci Part A: Polym Chem* 2019;57:1041-8. DOI
27. Xue Y, Xue Z, Zhang W, et al. Effects on optoelectronic performances of EDOT end-capped oligomers and electrochromic polymers by varying thienothiophene cores. *J Electroanal Chem* 2019;834:150-60. DOI
28. Zhu Z, Wang L, Gao C. Chapter3 - Thermoelectric properties of PEDOTs. Advanced PEDOT thermoelectric materials. *Elsevier*;2022. p. 73-95. DOI
29. Bubnova O, Khan ZU, Malti A, et al. Optimization of the thermoelectric figure of merit in the conducting polymer poly(3,4-ethylenedioxythiophene). *Nat Mater* 2011;10:429-33. DOI PubMed
30. Zhang Q, Sun Y, Xu W, Zhu D. Organic thermoelectric materials: emerging green energy materials converting heat to electricity directly and efficiently. *Adv Mater* 2014;26:6829-51. DOI
31. Beaujuge PM, Reynolds JR. Color control in pi-conjugated organic polymers for use in electrochromic devices. *Chem Rev* 2010;110:268-320. DOI PubMed
32. Corradi R, Armes S. Chemical synthesis of poly(3,4-ethylenedioxythiophene). *Synth Met* 1997;84:453-4. DOI
33. Pei Q, Zuccarello G, Ahlskog M, Inganäs O. Electrochromic and highly stable poly(3,4-ethylenedioxythiophene) switches between opaque blue-black and transparent sky blue. *Polymer* 1994;35:1347-51. DOI
34. Xiong J, Jiang F, Zhou W, Liu C, Xu J. Highly electrical and thermoelectric properties of a PEDOT:PSS thin-film via direct dilution - filtration. *RSC Adv* 2015;5:60708-12. DOI
35. Li X, Liu C, Zhou W, et al. Roles of polyethylenimine ethoxylated in efficiently tuning the thermoelectric performance of poly(3,4-ethylenedioxythiophene)-rich nanocrystal films. *ACS Appl Mater Interfaces* 2019;11:8138-47. DOI
36. Jia Y, Liu C, Liu J, et al. Efficient enhancement of the thermoelectric performance of vapor phase polymerized poly(3,4-ethylenedioxythiophene) films with poly(ethyleneimine). *J Polym Sci Part B: Polym Phys* 2019;57:257-65. DOI
37. Cho B, Park KS, Baek J, Oh HS, Koo Lee YE, Sung MM. Single-crystal poly(3,4-ethylenedioxythiophene) nanowires with ultrahigh conductivity. *Nano Lett* 2014;14:3321-7. DOI PubMed
38. Shen L, Liu P, Liu C, et al. Advances in efficient polymerization of solid-state trithiophenes for organic thermoelectric thin-film. *ACS Appl Polym Mater* 2020;2:376-84. DOI
39. Nicho ME, Hu H, López-Mata C, Escalante J. Synthesis of derivatives of polythiophene and their application in an electrochromic device. *Sol Energy Mater Sol Cells* 2004;82:105-18. DOI
40. Gök A, Omastová M, Yavuz AG. Synthesis and characterization of polythiophenes prepared in the presence of surfactants. *Synth Met* 2007;157:23-9. DOI
41. McCulloch I, Heeney M, Bailey C, et al. Liquid-crystalline semiconducting polymers with high charge-carrier mobility. *Nat Mater* 2006;5:328-33. DOI
42. Li M, Bai Z, Chen X, et al. Thermoelectric transport in conductive poly(3,4-ethylenedioxythiophene). *Chinese Phys B* 2022;31:027201. DOI
43. Lim E, Peterson KA, Su GM, Chabinyc ML. Thermoelectric properties of poly(3-hexylthiophene) (P3HT) doped with 2,3,5,6-tetrafluoro-7,7,8,8-tetracyanoquinodimethane (F_4TCNQ) by vapor-phase infiltration. *Chem Mater* 2018;30:998-1010. DOI
44. Wang S. Emerging efficient charge-transport landscape based on short-range order in conjugated polymers. *Synth Met* 2019;251:104-19. DOI
45. Perego G, Cella GD, Bastioli C. Effect of molecular weight and crystallinity on poly(lactic acid) mechanical properties. *J Appl Polym Sci* 1996;59:37-43. DOI
46. Stejskal J, Riede A, Hlavatá D, Prokeš J, Helmstedt M, Holler P. The effect of polymerization temperature on molecular weight, crystallinity, and electrical conductivity of polyaniline. *Synth Met* 1998;96:55-61. DOI
47. Ouyang J, Xu Q, Chu C, Yang Y, Li G, Shinar J. On the mechanism of conductivity enhancement in poly(3,4-ethylenedioxythiophene):poly(styrene sulfonate) film through solvent treatment. *Polymer* 2004;45:8443-50. DOI
48. Imae I, Shi M, Ooyama Y, Harima Y. Seebeck coefficients of poly(3,4-ethylenedioxythiophene):poly(styrene sulfonate) correlated with oxidation levels. *J Phys Chem C* 2019;123:4002-6. DOI
49. Kiefer D, Giovannitti A, Sun H, et al. Enhanced n-doping efficiency of a naphthalenediimide-based copolymer through polar side chains for organic thermoelectrics. *ACS Energy Lett* 2018;3:278-85. DOI PubMed PMC
50. Dubal DP, Chodankar NR, Kim DH, Gomez-Romero P. Towards flexible solid-state supercapacitors for smart and wearable electronics. *Chem Soc Rev* 2018;47:2065-129. DOI PubMed
51. Dyer A, Grenier C, Reynolds J. A Poly(3,4-alkylenedioxythiophene) Electrochromic variable optical attenuator with near-infrared reflectivity tuned independently of the visible region. *Adv Funct Mater* 2007;17:1480-6. DOI
52. Franke EB, Trimble CL, Hale JS, Schubert M, Woollam JA. Infrared switching electrochromic devices based on tungsten oxide. *J*

Appl Phys 2000;88:5777-84. DOI

53. Sekitani T, Zschieschang U, Klauk H, Someya T. Flexible organic transistors and circuits with extreme bending stability. *Nat Mater* 2010;9:1015-22. DOI PubMed
54. Fan Q, Su W, Guo X, et al. A 1,1′-vinylene-fused indacenodithiophene-based low bandgap polymer for efficient polymer solar cells. *J Mater Chem A* 2017;5:5106-14. DOI
55. Khodakarimi S, Hekhmatshoar MH, Nasiri M, Khaleghi Moghaddam M, Abbasi F. Effects of process and post-process treatments on the electrical conductivity of the PEDOT:PSS films. *J Mater Sci Mater Electron* 2016;27:1278-85. DOI